

Constraints on corrections to Newtonian gravity from two recent measurements of the Casimir interaction between metallic surfaces

G. L. Klimchitskaya,¹ U. Mohideen,² and V. M. Mostepanenko¹

¹*Central Astronomical Observatory at Pulkovo of the Russian Academy of Sciences, St.Petersburg, 196140, Russia*

²*Department of Physics and Astronomy, University of California, Riverside, California 92521, USA*

Abstract

We obtain constraints on parameters of the Yukawa-type corrections to Newton's gravitational law from measurements of the gradient of the Casimir force between surfaces coated with ferromagnetic metal Ni and from measurements of the Casimir force between Au-coated sinusoidally corrugated surfaces at various angles between corrugations. It is shown that constraints following from the experiment with magnetic surfaces are slightly weaker than currently available strongest constraints, but benefit from increased reliability and independence of systematic effects. The constraints derived from the experiment with corrugated surfaces within the interaction region from 11.6 to 29.2 nm are stronger up to a factor of 4 than the strongest constraints derived from other experiments. The possibility of further strengthening of constraints on non-Newtonian gravity by using the configurations with corrugated boundaries is proposed.

PACS numbers: 14.80.-j, 04.50.-h, 04.80.Cc, 12.20.Fv

I. INTRODUCTION

In the last few decades corrections to Newton's law of gravitation and constraints on them have become the subject of considerable study (see the monograph [1] and reviews [2–5]). From the experimental standpoint, it is of most importance that at separations between the test bodies below 0.1 mm Newton's law is not confirmed by measurements with sufficient precision. Theoretically, many extensions of the Standard Model of elementary particles and their interactions predict corrections to the Newton law of power- and Yukawa-type due to exchange of light and massless elementary particles [6–10]. On the other hand, similar corrections are predicted by the extra-dimensional physics with a low-energy compactification scale [11–15]. This makes the search for such corrections, or at least constraining their parameters, interesting for the problems of dark matter and unification of gravitation with other fundamental interactions.

A lot of successful work has been done on constraining the power- and Yukawa-type corrections to Newton's law of gravitation from gravitational experiments of Eötvös- and Cavendish-type [1–4, 16, 17]. Although the most strong constraints on the power-type corrections were obtained in this way, it was found that the resulting constraints on the Yukawa-type corrections become much weaker in the interaction range below a few micrometers. This is explained by the fact that at sufficiently small separations between the test bodies the van der Waals [18] and Casimir force [19] becomes the dominant background force in place of gravitation. The two names belong to a single force of quantum origin caused by the zero-point and thermal fluctuations of the electromagnetic field. They are usually used at short and relatively large separations, respectively, where the effects of relativistic retardation are immaterial or, on the contrary, are influential and should be taken into account.

The possibility to constrain corrections to Newton's law from the van der Waals and Casimir force was proposed long ago [20, 21] for the cases of Yukawa-type and power-type corrections, respectively. At that time, however, reasonably precise measurements of the van der Waals and Casimir force were not available. Things have changed during the last 15 years when a lot of more precise experiments on measuring the Casimir force between metallic, dielectric and semiconductor bodies have been performed (see reviews [22–25]). The measure of agreement between the measurement data of these experiments and theoretical description

of the Casimir force in the framework of the Lifshitz theory resulted in the strengthening of previously known constraints on the parameters of Yukawa-type corrections up to a factor of 2.4×10^7 [5, 19, 26]. Using different experiments on measurement of the Casimir force, the strongest constraints on the corrections to Newton's law were obtained over a wide interaction region from about 1 nm to a few micrometers. Note that for shorter interaction regions the strongest constraints on the Yukawa-type corrections follow from precise atomic physics [27], whereas starting from a few micrometers the gravitational experiments [1–4, 16, 17] remain the most reliable source of such constraints.

In this paper we obtain constraints on the Yukawa-type corrections to Newton's gravitational law from two recently performed experiments on measuring the Casimir interaction by means of an atomic force microscope (AFM). Each of these experiments is highly significant, as compared with all earlier measurements of the Casimir interaction. In the first [28] the dynamic AFM was used to measure the gradient of the Casimir force between a plate and a sphere both coated with the ferromagnetic metal Ni with no spontaneous magnetization. As a result, the predictions of the Lifshitz theory generalized for the case of magnetic materials more than 40 years ago [29] were experimentally confirmed. The distinguished feature of the experiment with two magnetic surfaces is also that it allows to shed light on the role of some important systematic effects (see Sec. II for details) and, thus, remove any doubt in the reliability of constraints obtained.

In the second experiment of our interest here [30] the static AFM was used to measure the Casimir force between a plate and a sphere both with sinusoidally corrugated surfaces coated with nonmagnetic metal Au. The unusual feature of this experiment, as compared with earlier performed experiments with corrugated surfaces, is that the Casimir force was measured at various angles between the longitudinal corrugations on both bodies. This introduced into the problem an additional parameter (the angle between corrugations) that can be chosen to obtain the most strong constraints from the measure of agreement between the experimental data and theory of the Casimir force for corrugated surfaces based on the derivative expansion [31–33].

The constraints on corrections to Newton's law obtained by us from the experiment with magnetic surfaces are in agreement with those obtained earlier [34] for smooth Au surfaces by means of dynamic AFM [35], but slightly weaker due to different densities of Au and Ni. The advantage of constraints following from the experiment with Ni surfaces is that they

are not only fully justified on their own, but add substantiation to the constraints obtained from the experiments with nonmagnetic metal surfaces. As to constraints obtained from the experiment with corrugated surfaces, they are stronger up to a factor of 4 than the most strong constraints reported so far [26, 36, 37] in the interaction region from 11.6 to 29.2 nm.

The paper is organized as follows. In Sec. II we present the exact expression for the Yukawa-type interaction in the experimental configuration of Ref. [28] and derive the respective constraints on corrections to Newton's gravitational law. The advantages of using magnetic materials are elucidated. Section III is devoted to the experiment with corrugated surfaces [30]. Here, we derive an expression for the Yukawa-type force in configurations with different angles between corrugations. The obtained expression is used to find the stronger constraints on corrections to Newton's law. Some modifications in the setup are proposed allowing further strengthening of the constraints in configurations with corrugated surfaces. In Sec. IV the reader will find our conclusions and discussion.

II. CONSTRAINTS FROM THE GRADIENT OF THE CASIMIR FORCE BETWEEN TWO MAGNETIC SURFACES

We begin with the standard parametrization of the spin-independent Yukawa-type correction to Newton's gravitational law [1–5] (for spin-dependent corrections see Refs. [38, 39]). The total gravitational potential between the two point-like masses m_1 and m_2 spaced at a separation r takes the form

$$V(r) = V_N(r) + V_{\text{Yu}}(r) = -\frac{Gm_1m_2}{r} (1 + \alpha e^{-r/\lambda}), \quad (1)$$

where $V_N(r)$ and $V_{\text{Yu}}(r)$ are the Newtonian part and the Yukawa-type correction, respectively. Here, G is the Newtonian gravitational constant, and α and λ are the strength and interaction range of the Yukawa-type correction. Similar to Ref. [40] it can be shown that at separations below a few micrometers the Newtonian gravitational force between the test bodies V_1 and V_2 in experiments under consideration is much smaller than the error in measurements of the Casimir force. Because of this, in all subsequent calculations the Newtonian potential can be neglected, and the Yukawa-type addition to it is considered on the background of the measured Casimir force. Then the gravitational force acting between the test bodies at short separations can be obtained by the integration of the Yukawa-type

correction $V_{\text{Yu}}(r)$ defined in Eq. (1) over the volumes of both bodies

$$V_{\text{Yu}}(a) = -G\alpha \int_{V_1} d^3r_1 \rho_1(\mathbf{r}_1) \int_{V_2} d^3r_2 \rho_2(\mathbf{r}_2) \frac{e^{-|\mathbf{r}_1 - \mathbf{r}_2|/\lambda}}{|\mathbf{r}_1 - \mathbf{r}_2|}. \quad (2)$$

Here, a is the closest separation between the test bodies and $\rho_1(\mathbf{r}_1)$ and $\rho_2(\mathbf{r}_2)$ are the respective mass densities (note that ρ_1 and ρ_2 are not constant because in the experiments used below each test body consists of several homogeneous layers of different densities). The gravitational force due to the Yukawa-type correction and its gradient are given by

$$F_{\text{Yu}}(a) = -\frac{\partial V_{\text{Yu}}(a)}{\partial a}, \quad \frac{\partial F_{\text{Yu}}(a)}{\partial a} = -\frac{\partial^2 V_{\text{Yu}}(a)}{\partial a^2}. \quad (3)$$

In the experiment [28] the gradient of the Casimir force was measured between a Ni-coated plate and a Ni-coated hollow microsphere attached to the tip of an AFM cantilever operated in the dynamic regime [19, 22]. The silicon plate (V_1) of a few millimeter diameter and thickness can be considered as having an infinitely large area and an infinitely large thickness when we have to deal with the submicrometer region of λ . The density of Si is $\rho_{\text{Si}} = 2.33 \times 10^3 \text{ kg/m}^3$. For technological purposes the Si plate was coated first with a layer of Cr having a thickness $\Delta_{\text{Cr}}^{(1)} = 10 \text{ nm}$ and density $\rho_{\text{Cr}} = 7.15 \times 10^3 \text{ kg/m}^3$ and then with a layer of Al having a thickness $\Delta_{\text{Al}}^{(1)} = 40 \text{ nm}$ and density $\rho_{\text{Al}} = 2.7 \times 10^3 \text{ kg/m}^3$. Finally the plate was coated with an outer layer of magnetic metal Ni with a thickness $\Delta_{\text{Ni}}^{(1)} = 250 \text{ nm}$ and density $\rho_{\text{Ni}} = 8.9 \times 10^3 \text{ kg/m}^3$. The hollow microsphere (V_2) was made of glass with density $\rho_g = 2.5 \times 10^3 \text{ kg/m}^3$. The thickness of the spherical envelope was $\Delta_g^{(2)} = 5 \mu\text{m}$. The sphere was also coated with successive layers of Cr, Al and Ni having the thicknesses $\Delta_{\text{Cr}}^{(2)} = \Delta_{\text{Cr}}^{(1)}$, $\Delta_{\text{Al}}^{(2)} = \Delta_{\text{Al}}^{(1)}$, and $\Delta_{\text{Ni}}^{(2)} = 210 \text{ nm}$. The outer radius of the sphere with all the coatings included is $R = 61.7 \mu\text{m}$.

The exact integration over the volumes of a plate and a sphere in Eq.(2) with account of their layer structure can be performed like in Ref. [41]. Then, substituting the obtained result in Eq. (3), we arrive at

$$\frac{\partial F_{\text{Yu}}(a)}{\partial a} = 4\pi^2 G\alpha \lambda^2 e^{-a/\lambda} X^{(1)}(\lambda) X^{(2)}(\lambda), \quad (4)$$

where the following notations are introduced:

$$\begin{aligned}
X^{(1)}(\lambda) &= \rho_{\text{Ni}} - (\rho_{\text{Ni}} - \rho_{\text{Al}})e^{-\Delta_{\text{Ni}}^{(1)}/\lambda} \\
&\quad - (\rho_{\text{Al}} - \rho_{\text{Cr}})e^{-(\Delta_{\text{Ni}}^{(1)} + \Delta_{\text{Al}}^{(1)})/\lambda} \\
&\quad - (\rho_{\text{Al}} - \rho_{\text{Si}})e^{-(\Delta_{\text{Ni}}^{(1)} + \Delta_{\text{Al}}^{(1)} + \Delta_{\text{Cr}}^{(1)})/\lambda}, \\
X^{(2)}(\lambda) &= \rho_{\text{Ni}}\Phi(R, \lambda) - (\rho_{\text{Ni}} - \rho_{\text{Al}})\Phi(R - \Delta_{\text{Ni}}^{(2)}, \lambda)e^{-\Delta_{\text{Ni}}^{(2)}/\lambda} \\
&\quad - (\rho_{\text{Al}} - \rho_{\text{Cr}})\Phi(R - \Delta_{\text{Ni}}^{(2)} - \Delta_{\text{Al}}^{(2)}, \lambda)e^{-(\Delta_{\text{Ni}}^{(2)} + \Delta_{\text{Al}}^{(2)})/\lambda} \\
&\quad - (\rho_{\text{Cr}} - \rho_g)\Phi(R - \Delta_{\text{Ni}}^{(2)} - \Delta_{\text{Al}}^{(2)} - \Delta_{\text{Cr}}^{(2)}, \lambda)e^{-(\Delta_{\text{Ni}}^{(2)} + \Delta_{\text{Al}}^{(2)} + \Delta_{\text{Cr}}^{(2)})/\lambda} \\
&\quad - \rho_g\Phi(R - \Delta_{\text{Ni}}^{(2)} - \Delta_{\text{Al}}^{(2)} - \Delta_{\text{Cr}}^{(2)} - \Delta_g^{(2)}, \lambda)e^{-(\Delta_{\text{Ni}}^{(2)} + \Delta_{\text{Al}}^{(2)} + \Delta_{\text{Cr}}^{(2)} + \Delta_g^{(2)})/\lambda},
\end{aligned} \tag{5}$$

and the following notation is introduced

$$\Phi(r, \lambda) = r - \lambda + (r + \lambda)e^{-2r/\lambda}. \tag{6}$$

The constraints on the parameters (λ, α) , which are often referred to as the parameters of *non-Newtonian gravity*, can be obtained from the comparison between the measurement data for the gradient of the Casimir force $F'_C(a)$ and respective theory. In Ref. [28] it was found that within the entire separation region from 223 to 550 nm there is an excellent agreement between the data and theoretical predictions of the Lifshitz theory of the van der Waals and Casimir force [18, 19] with omitted relaxation properties of conduction electrons (the so-called *plasma model approach*). The predictions of the Lifshitz theory with included relaxation properties of free charge carriers (the so-called *Drude model approach*) were excluded by the measurement data at a 95% confidence level within the separation region from 223 to 350 nm (in the end of this section we provide a brief discussion of different approaches to the Lifshitz theory which is essential for obtaining constraints on non-Newtonian gravity). The measure of agreement with the adequate theory is characterized by the total experimental error $\Delta_{F'_C}(a)$ in the measured gradient of the Casimir force determined at a 67% confidence level [28]. Keeping in mind that within the limits of this error no additional interaction of Yukawa-type was observed, the constraints on the parameters λ and α can be obtained from the inequality

$$\left| \frac{\partial F_{\text{Yu}}(a)}{\partial a} \right| \leq \Delta_{F'_C}(a). \tag{7}$$

We have substituted Eqs. (4)–(6) in Eq. (7) and analyzed the resulting inequality at different separations. It was found that for $\lambda \lesssim 200$ nm the strongest constraints are determined at

the shortest separation $a = 223$ nm where $\Delta_{F'_C} = 1.2 \mu\text{N/m}$ [28]. For $200 \text{ nm} \lesssim \lambda \lesssim 315$ nm and $315 \text{ nm} \lesssim \lambda \lesssim 630$ nm the strongest constraints follow at $a = 250$ and 300 nm, respectively (with respective $\Delta_{F'_C} = 1.05$ and $0.89 \mu\text{N/m}$). Finally, at $\lambda > 630$ nm the strongest constraints are obtained at $a = 350$ nm ($\Delta_{F'_C} = 0.81 \mu\text{N/m}$). The resulting constraints are shown by the solid line in Fig. 1. Here and below the region of (λ, α) plane above each line is prohibited and below is allowed by the results of respective experiment. In the same figure by the dashed line we show the constraints obtained in Ref. [34] from measurements of the gradient of the Casimir force between two Au-coated surfaces by means of dynamic AFM [35]. The dotted line shows the constraints obtained [34] from the experiment on measuring gradient of the Casimir force between an Au-coated sphere and a Ni-coated plate [42] using the same setup. As can be seen in Fig. 1, the constraints indicated by the solid line are slightly weaker than those shown by the dashed and dotted lines. This is caused by the fact that density of Ni is smaller than density of Au and by different experimental errors. Note also that our constraints shown by the solid line can be obtained in a simpler way by using the proximity force approximation [19, 22]

$$F_{\text{Yu}}(a) = 2\pi R E_{\text{Yu}}(a), \quad (8)$$

to calculate the gradient of the Yukawa-type force, where $E_{\text{Yu}}(a)$ is the energy per unit area of Yukawa-type interaction between two plane-parallel plates having the same layer structure as our test bodies. According to the results of Refs. [41, 43], this is possible under the conditions

$$\frac{\lambda}{R} \ll 1, \quad \frac{\Delta_{\text{Au}}^{(2)} + \Delta_{\text{Al}}^{(2)} + \Delta_{\text{Cr}}^{(2)} + \Delta_g^{(2)}}{R} \ll 1, \quad (9)$$

which are satisfied in our experimental configuration with a wide safety margin. In this case the function $\Phi(r, \lambda)$ with any argument r can be approximately replaced with R .

It would be interesting also to compare the constraints on non-Newtonian gravity obtained here from the experiment with two Ni surfaces (solid line in Fig. 1) with the strongest constraints obtained so far using the alternative setups. For this purpose in Fig. 2 we reproduce the solid line of Fig. 1 as the solid line 1. The solid line 2 in Fig. 2 was obtained [26] from measurements of the thermal Casimir-Polder force between ^{87}Pb atoms belonging to the Bose-Einstein condensate and a SiO_2 plate [44], and the solid line 3 was obtained [45] from measurements of gradient of the Casimir force between an Au sphere and a rectangular corrugated semiconductor (Si) plate by means of a micromachined oscillator [46]. Next, the

solid line 4 in Fig. 2 was found from an effective measurement of the Casimir pressure between two parallel Au plates by means of a micromachined oscillator [36, 37], and the dashed line was obtained from the Casimir-less experiment [47]. As can be seen in Fig. 2, various constraints obtained using quite different setups are consistent with the constraints of line 1 obtained from the most recent experiment with two magnetic surfaces.

In the end of this section it is pertinent to note that the experiment with two magnetic surfaces [28] plays the key role in the test of validity of the Lifshitz theory. Keeping in mind that constraints on non-Newtonian gravity are derived from the measure of agreement between the measurement data and theory, this experiment is also important to validate the reliability of constraints obtained. As mentioned above, the Lifshitz theory is in agreement with the plasma model approach to the Casimir force, which disregards the relaxation properties of free charge carriers, and excludes the Drude model approach taking these properties into account (see the experiments of Refs. [35–37] and earlier experiments reviewed in Refs. [19, 22]). This is against expectations of many and gave rise to the search of some systematic effects which could reverse the situation. After several unsuccessful attempts (see Ref. [48] for a review) the influence of large surface patches was selected as the most probable systematic effect which could bring the data in agreement with the Drude model approach [49]. In two experiments on measuring the Casimir force between Au surfaces [50, 51] hypothetical large patches were described by models with free fitting parameters and used in respective fitting procedures. In these experiments, which are not independent measurements of the Casimir force, an agreement of the data with the Drude model approach has been claimed (see Refs. [52–56] for a critical discussion).

The crucial point to underline here is that for nonmagnetic metals the Drude model approach leads to smaller gradients of the Casimir force than the plasma model approach [19, 22, 35–37]. Thus, the effect of large patch potentials (which leads to an attraction similar to the Casimir force) is added to the predictions of the Drude model approach and might make the total theoretical force compatible with the measurement data [49]. By contrast, for two magnetic metals the Drude model approach leads to larger gradients of the Casimir force than the plasma model approach [28, 57, 58]. Thus, if the effect of patches were important in this case, it would further increase the disagreement between the predictions of the Drude model approach and the measurement data observed in Ref. [28]. This confirms that surface patches do not play an important role in precise experiments on measuring the Casimir force

in accordance with the model of patches [59] predicting a negligibly small effect from patches [19, 22]. Recently the patches on Au samples used in measurements of the Casimir force were investigated by means of Kelvin probe microscopy [60]. The force originating from them was found to be too small to affect the conclusions following from precise measurements of the Casimir force. It is the matter of fact that the experimental data of all independent measurements of the Casimir interaction between both nonmagnetic and magnetic metals are in excellent agreement with the predictions of the Lifshitz theory combined with the plasma model approach and exclude the Drude model approach. Although the fundamental reasons behind this fact have not yet been finally understood, the constraints on non-Newtonian gravity obtained on this basis can be already considered as reliable enough.

III. CONSTRAINTS FROM THE CASIMIR FORCE BETWEEN TWO CORRUGATED SURFACES

In Sec. II we have used the most recent measurement of the Casimir interaction where the material dependence played a major role in theory-experiment comparison. Another recent experiment [30] is of quite a different nature. In Ref. [30] the normal Casimir force acting perpendicular to the surface was measured between the sinusoidally corrugated surfaces of a sphere and a plate. The corrugated boundary surfaces have long been used in measurements of the Casimir force (see Refs. [22, 23] for a review). For example, the normal Casimir force between a rectangular corrugated semiconductor (Si) plate and a smooth Au sphere has been measured by means of a micromachined oscillator and compared with theory based on the exact scattering approach [46]. The obtained constraints on non-Newtonian gravity are discussed in Sec. II (see solid line 3 in Fig. 2). A further example is the lateral Casimir force between a sinusoidally corrugated plate and a sinusoidally corrugated sphere, both coated with Au, which was measured and compared with exact theory in Refs. [61, 62]. This experiment resulted in the maximum strengthening of constraints on non-Newtonian gravity from the Casimir effect by a factor of 2.4×10^7 discussed in Sec. I. In experiments with corrugated surfaces the nontrivial geometry plays a major role in the theory-experiment comparison whereas different approaches to the description of material properties cannot be differentiated due to the lower experimental precision.

The specific feature of the experiment of Ref. [30] is that the normal Casimir force between

a sinusoidally corrugated Au-coated plate and a sinusoidally corrugated Au-coated sphere was measured at various angles between corrugations using an AFM. The plate in this experiment is the diffraction grating with uniaxial sinusoidal corrugations of period $\Lambda = 570.5$ nm and amplitude $A_1 = 40.2$ nm. The grating was made of hard epoxy with density $\rho_e = 1.08 \times 10^3$ kg/m³ and coated with an Au layer of thickness $\Delta_{\text{Au}}^{(1)} = 300$ nm. The corrugated plate was used as a template for the pressure imprinting of the corrugations on the bottom surface of a sphere. The polystyrene sphere has a density $\rho_p = 1.06 \times 10^3$ kg/m³. It was coated with a layer of Cr of thickness $\Delta_{\text{Cr}}^{(2)} = 10$ nm, then with a layer of Al of thickness $\Delta_{\text{Al}}^{(2)} = 20$ nm and finally with a layer of Au of thickness $\Delta_{\text{Au}}^{(2)} = 110$ nm. The outer radius of the coated sphere is $R = 99.6$ μm . The imprinted corrugations on the sphere have the same period as on the plate and the amplitude $A_2 = 14.6$ nm. The size of an imprint area was measured to be $L_x \approx L_y \approx 14$ μm , i.e., it is much larger than Λ . In Ref. [30] the Casimir force between the sphere and the plate was measured at the following angles between the axes of corrugations on both bodies: $\theta = 0^\circ, 1.2^\circ, 1.8^\circ, \text{ and } 2.4^\circ$.

Now we calculate the Yukawa-type force in the experimental configuration of Ref. [30]. For this purpose we first consider the Yukawa-type energy per unit area in the configuration of two plane-parallel plates spaced at a separation a having the same layer structure as a plate and a sphere in the experiment. The result is [41]

$$E_{\text{Yu}}(a) = -2\pi G\alpha\lambda^3 e^{-a/\lambda} X^{(1)}(\lambda)X^{(2)}(\lambda), \quad (10)$$

where now

$$\begin{aligned} X^{(1)}(\lambda) &= \rho_{\text{Au}} - (\rho_{\text{Au}} - \rho_e)e^{-\Delta_{\text{Au}}^{(1)}/\lambda}, \\ X^{(2)}(\lambda) &= \rho_{\text{Au}} - (\rho_{\text{Au}} - \rho_{\text{Al}})e^{-\Delta_{\text{Au}}^{(2)}/\lambda} \\ &\quad - (\rho_{\text{Al}} - \rho_{\text{Cr}})e^{-(\Delta_{\text{Au}}^{(2)} + \Delta_{\text{Al}}^{(2)})/\lambda} \\ &\quad - (\rho_{\text{Cr}} - \rho_p)e^{-(\Delta_{\text{Au}}^{(2)} + \Delta_{\text{Al}}^{(2)} + \Delta_{\text{Cr}}^{(2)})/\lambda}. \end{aligned} \quad (11)$$

Next, we introduce corrugations at an angle θ on the parallel plates and find their effect by means of the geometrical averaging [19, 22]

$$E_{\text{Yu}}^{\text{corr}}(a) = \frac{1}{L_x L_y} \int_{-L_x/2}^{L_x/2} dx \int_{-L_y/2}^{L_y/2} dy E_{\text{Yu}}(z(a, x, y)). \quad (12)$$

Here, E_{Yu} is the energy per unit area defined in Eq. (10) calculated at different separations

z between the corrugated plates which are assumed parallel to the (x, y) plane

$$z(a, x, y) = a + A_1 \cos \frac{2\pi x}{\Lambda} - A_2 \cos \frac{2\pi x'}{\Lambda}. \quad (13)$$

Note that there is no phase shift between the corrugations on both plates, so that $x' = x \cos \theta - y \sin \theta$.

Finally, to obtain the Yukawa-type force between a corrugated plate and a corrugated sphere, we apply the proximity force approximation (8) taking into account different radii of separate spherical layers. After an easy calculation using Eqs. (10)–(13), the Yukawa-type force between a corrugated plate and a corrugated sphere takes the form

$$F_{\text{Yu}}^{\text{corr}}(a) = -4\pi^2 G \alpha \lambda^3 e^{-a/\lambda} X^{(1)}(\lambda) \tilde{X}^{(2)}(\lambda) X(\lambda, \theta), \quad (14)$$

where

$$\begin{aligned} \tilde{X}^{(2)}(\lambda) &= R\rho_{\text{Au}} - (\rho_{\text{Au}} - \rho_{\text{Al}})(R - \Delta_{\text{Au}}^{(2)})e^{-\Delta_{\text{Au}}^{(2)}/\lambda} \\ &\quad - (\rho_{\text{Al}} - \rho_{\text{Cr}})(R - \Delta_{\text{Au}}^{(2)} - \Delta_{\text{Al}}^{(2)})e^{-(\Delta_{\text{Au}}^{(2)} + \Delta_{\text{Al}}^{(2)})/\lambda} \\ &\quad - (\rho_{\text{Cr}} - \rho_p)(R - \Delta_{\text{Au}}^{(2)} - \Delta_{\text{Al}}^{(2)} - \Delta_{\text{Cr}}^{(2)})e^{-(\Delta_{\text{Au}}^{(2)} + \Delta_{\text{Al}}^{(2)} + \Delta_{\text{Cr}}^{(2)})/\lambda} \end{aligned} \quad (15)$$

and the function $X(\lambda, \theta)$ is defined as

$$X(\lambda, \theta) = \frac{1}{L_x L_y} \int_{-L_x/2}^{L_x/2} dx \int_{-L_y/2}^{L_y/2} dy e^{-[A_1 \cos(2\pi x/\Lambda) - A_2 \cos(2\pi x'/\Lambda)]/\lambda}. \quad (16)$$

For zero angle between corrugations at both surfaces ($\theta = 0$) one arrives to a more simple representation

$$X(\lambda, 0) = \frac{1}{L_x} \int_{-L_x/2}^{L_x/2} dx e^{-[(A_1 - A_2) \cos(2\pi x/\Lambda)]/\lambda}. \quad (17)$$

The integral in Eq. (17) can be evaluated analytically using the formula 2.5.10(3) in Ref. [63] if there is an integer n such that $n\Lambda = L_x$. In this case

$$X(\lambda, 0) = I_0 \left(\frac{A_1 - A_2}{\lambda} \right), \quad (18)$$

where $I_0(z)$ is the Bessel function of imaginary argument. If $n\Lambda + \eta = L_x$ where $0 < \eta < \Lambda$, Eq. (18) is satisfied only approximately. If in the interaction region of our interest (see Fig. 4 below) it occurs $(A_1 - A_2)/\lambda \gg 1$, the maximum error arising from the use of Eq. (18) achieves 5%. In the case $(A_1 - A_2)/\lambda \sim 1$ this error is equal to $\approx 2\%$. In the general case of an arbitrary θ the quantity $X(\lambda, \theta)$ can be computed numerically. In Fig. 3

the computational results are plotted by the solid lines as functions of λ at $\theta = 0^\circ, 1.2^\circ, 1.8^\circ$, and 2.4° used in the experiment of Ref. [30] from bottom to top, respectively, to a logarithmic scale.

The measurement data of Ref. [30] for the normal Casimir force between corrugated surfaces were compared with the results of numerical computations based on the derivative expansion approach [31–33] and a good agreement was found within the limits of the experimental errors $\Delta_{F_C}(a)$ determined at the 67% confidence level (minor disagreement at the shortest separations in Fig. 3 of Ref. [30] comes from the use of an oscillator model in place of the optical data for the complex index of refraction). Then the constraints on the parameters λ and α of the corrections to Newton’s law were found from the inequality

$$|F_{\text{Yu}}(a)| \leq \Delta_{F_C}(a), \quad (19)$$

where $F_{\text{Yu}}(a)$ is given by Eq. (14) with the notations in Eqs. (11), (15) and (16). We have numerically analyzed Eq. (19) at different separations a and with different values of the angle θ between corrugations. The strongest constraints were obtained at the shortest separation $a = 127$ nm where $\Delta_{F_C} = 0.94$ pN. They are shown by the solid lines in Figs. 4(a)–4(d) at the values of $\theta = 0^\circ, 1.2^\circ, 1.8^\circ$, and 2.4° , respectively. For comparison purposes, the dashed lines 1 and 2 in Figs. 4(a)–4(d) show the strongest constraints obtained earlier [26] within this interaction region from measurements of the lateral Casimir force between sinusoidally corrugated surfaces [61, 62] and from effective measurements of the Casimir pressure between metallic plates by means of a micromachined oscillator [36, 37]. As can be seen in Fig. 4, at any θ measurements of the normal Casimir force between sinusoidally corrugated surfaces result in stronger constraints within some interaction region than were known so far. Thus at $\theta = 0^\circ$ the strengthening of previously available constraints up to a factor 1.8 holds within the interaction region $14.3 \text{ nm} \leq \lambda \leq 19.5 \text{ nm}$ with the largest strengthening achieved at $\lambda = 17.2 \text{ nm}$ [see Fig. 4(a)]. At $\theta = 1.2^\circ$ and 1.8° the strengthening up to factors 2.8 and 3.5 occurs for $13.8 \text{ nm} \leq \lambda \leq 25.1 \text{ nm}$ and $12.9 \text{ nm} \leq \lambda \leq 27.5 \text{ nm}$, respectively. The maximum strengthening up to a factor 4 (achieved at $\lambda = 17.2 \text{ nm}$) within the interaction region $11.6 \text{ nm} \leq \lambda \leq 29.2 \text{ nm}$ takes place at the angle between corrugations $\theta = 2.4^\circ$.

The obtained stronger constraints following from measurements of the normal Casimir force between sinusoidally corrugated surfaces can be further strengthened at the expense of some modification of the experimental setup. Thus, it would be useful to switch from

a static AFM mode used in this experiment to the dynamic mode used in Refs. [28, 35, 42]. This results in a higher experimental precision though makes it necessary to perform measurements at larger separation distances. As an example, we calculate the prospective constraints on λ, α which can be obtained from dynamic measurements of the gradient of the Casimir force between corrugated surfaces at $a = 170$ nm. In so doing we assume that the total experimental error obtainable at this experiment is $\Delta_{F'_C} = 0.62 \mu\text{N/m}$. For the sake of simplicity we consider the case $\theta = 0^\circ$ which does not lead to the maximum strengthening of the respective constraints. Then from Eq. (14) one obtains

$$\frac{\partial F_{\text{Yu}}^{\text{corr}}(a)}{\partial a} = 4\pi^2 G\alpha\lambda^2 e^{-a/\lambda} X^{(1)}(\lambda)\tilde{X}^{(2)}(\lambda)X(\lambda, 0). \quad (20)$$

Substituting Eq. (20) in the left-hand side of Eq. (7) adapted for the case of corrugated surfaces, we arrive at the prospective constraints shown by the dotted line in Fig. 5. In the same figure the strongest constraints obtained [26] from measurements of the lateral Casimir force between sinusoidally corrugated surfaces [61, 62], from effective measurements of the Casimir pressure between metallic plates by means of a micromachined oscillator [36, 37], and from the Casimir-less experiment [47] are indicated by the dashed lines 1, 2, and 3, respectively. As can be seen in Fig. 5, the prospective constraints shown by the dotted line are stronger than the strongest current constraints over a wide interaction region from 12 to 160 nm. At the moment three different experiments are used to constrain the Yukawa-type corrections to Newton's law within this interaction region. The maximum strengthening up to a factor of 12.6 occurs at $\lambda = 17.2$ nm.

IV. CONCLUSIONS AND DISCUSSION

In the foregoing we have obtained constraints on the parameters of Yukawa-type corrections to Newton's law of gravitation following from two recent experiments on measuring the Casimir interaction. Each of these experiments is of particular interest, as compared with all previous work in the field. The experiment of Ref. [28] pioneered measuring the gradient of the Casimir force between two magnetic surfaces and confirmed the predictions of the Lifshitz theory combined with the plasma model approach. In this way it was demonstrated that magnetic properties of the material boundaries influence the Casimir force. The outstanding property of magnetic materials is that the force gradients predicted by

the Drude model approach are larger than those predicted by the plasma model approach (just opposite to the case of nonmagnetic metals). Thus, it was confirmed that such a widely discussed systematic effect as the patch potentials cannot be used for the reconciliation of the measurement data with the Drude model approach leading to further support of constraints on non-Newtonian gravity obtained from the measure of agreement between experiment and theory. Although constraints following from the experiment with magnetic surfaces are slightly weaker than the previously known ones (this is due to smaller density of Ni as compared to Au), the increased reliability can be considered as an advantage.

The experiment of Ref. [30] pioneered measurements of the normal Casimir force between metallized sinusoidally corrugated surfaces at various angles between corrugations. It was demonstrated that the Casimir force depends on these angles in accordance with theory using the derivative expansion. We have calculated the Yukawa-type force in the experimental configuration with corrugated surfaces and obtained the respective constraints on its parameters. It was shown that the strength of constraints increases with increasing angle between corrugations. The maximum strengthening up to a factor of 4, as compared to the strongest previously known constraints, was shown to occur within the interaction range from 11.6 to 29.2 nm. We have also proposed some modification in the measurement scheme allowing strengthening of the previously known constraints up to a factor of 12.6 within a wide interaction region presently covered using the results of three different experiments. This means that measurements of the Casimir interaction retain considerable potential for further strengthening of constraints on the Yukawa-type corrections to Newton's gravitational law in submicrometer interaction region.

Acknowledgments

This work was supported by the NSF Grant No. PHY0970161 and DOE grant DEF010204ER46131 (U.M.).

[1] E. Fischbach and C. L. Talmadge, *The Search for Non-Newtonian Gravity* (Springer, New York, 1999).

- [2] E. G. Adelberger, B. R. Heckel, C. W. Stubbs, and W. F. Rogers, *Ann. Rev. Nucl. Part. Sci.* **41**, 269 (1991).
- [3] E. G. Adelberger, B. R. Heckel, and A. E. Nelson, *Ann. Rev. Nucl. Part. Sci.* **53**, 77 (2003).
- [4] E. G. Adelberger, J. H. Gundlach, B. R. Heckel, S. Hoedl, and S. Schlamminger, *Progr. Part. Nucl. Phys.* **62**, 102 (2009).
- [5] V. M. Mostepanenko, V. B. Bezerra, G. L. Klimchitskaya, and C. Romero, *Int. J. Mod. Phys. A* **27**, 1260015 (2012).
- [6] R. D. Peccei and H. R. Quinn, *Phys. Rev. Lett.* **38**, 1440 (1977).
- [7] S. Ferrara, J. Scherk, and B. Zumino, *Nucl. Phys. B* **121**, 393 (1977).
- [8] Y. Fujii, *Int. J. Mod. Phys. A* **6**, 3505 (1991).
- [9] S. Deser and B. Zumino, *Phys. Rev. Lett.* **38**, 1433 (1977).
- [10] S. Dimopoulos and G. F. Giudice, *Phys. Lett. B* **379**, 105 (1996).
- [11] I. Antoniadis, N. Arkani-Hamed, S. Dimopoulos, and G. Dvali, *Phys. Lett. B* **436**, 257 (1998).
- [12] N. Arkani-Hamed, S. Dimopoulos, and G. Dvali, *Phys. Lett. B* **429**, 263 (1998).
- [13] N. Arkani-Hamed, S. Dimopoulos, and G. Dvali, *Phys. Rev. D* **59**, 086004 (1999).
- [14] E. G. Floratos and G. K. Leontaris, *Phys. Lett. B* **465**, 95 (1999).
- [15] A. Kehagias and K. Sfetsos, *Phys. Lett. B* **472**, 39 (2000).
- [16] S. J. Smullin, A. A. Geraci, D. M. Weld, J. Chiaverini, S. Holmes, and A. Kapitulnik, *Phys. Rev. D* **72**, 122001 (2005).
- [17] A. A. Geraci, S. J. Smullin, D. M. Weld, J. Chiaverini, and A. Kapitulnik, *Phys. Rev. D* **78**, 022002 (2008).
- [18] V. A. Parsegian, *Van der Waals Forces: A Handbook for Biologists, Chemists, Engineers, and Physicists* (Cambridge University Press, Cambridge, 2005).
- [19] M. Bordag, G. L. Klimchitskaya, U. Mohideen, and V. M. Mostepanenko, *Advances in the Casimir Effect* (Oxford University Press, Oxford, 2009).
- [20] V. A. Kuzmin, I. I. Tkachev, and M. E. Shaposhnikov, *Pis'ma v ZhETF* **36**, 49 (1982) [*JETP Lett.* **36**, 59 (1982)].
- [21] V. M. Mostepanenko and I. Yu. Sokolov, *Phys. Let. A* **125**, 405 (1987).
- [22] G. L. Klimchitskaya, U. Mohideen, and V. M. Mostepanenko, *Rev. Mod. Phys.* **81**, 1827 (2009).
- [23] G. L. Klimchitskaya, U. Mohideen, and V. M. Mostepanenko, *Int. J. Mod. Phys. B* **25**, 171

- (2011).
- [24] A. W. Rodriguez, F. Capasso, and S. G. Johnson, *Nature Photonics* **5**, 211 (2011).
 - [25] R. Onofrio, *New J. Phys.* **8**, 237 (2006).
 - [26] V. B. Bezerra, G. L. Klimchitskaya, V. M. Mostepanenko, and C. Romero, *Phys. Rev. D* **81**, 055003 (2010).
 - [27] S. G. Karshenboim, *Phys. Rev. D* **82**, 073003 (2010).
 - [28] A. A. Banishev, G. L. Klimchitskaya, V. M. Mostepanenko, and U. Mohideen, *Phys. Rev. Lett.* **110**, 137401 (2013).
 - [29] P. Richmond and B. W. Ninham, *J. Phys. C: Solid St. Phys.* **4**, 1988 (1971).
 - [30] A. A. Banishev, J. Wagner, T. Emig, R. Zandi, and U. Mohideen, *Phys. Rev. Lett.* **110**, 250403 (2013).
 - [31] C. D. Fosco, F. C. Lombardo, and F. D. Mazzitelli, *Phys. Rev. D* **84**, 105031 (2011).
 - [32] G. Bimonte, T. Emig, R. L. Jaffe, and M. Kardar, *Europhys. Lett.* **97**, 50001 (2012).
 - [33] G. Bimonte, T. Emig, and M. Kardar, *Appl. Phys. Lett.* **100**, 074110 (2012).
 - [34] G. L. Klimchitskaya, U. Mohideen, and V. M. Mostepanenko, *Phys. Rev. D* **86**, 065025 (2012).
 - [35] C.-C. Chang, A. A. Banishev, R. Castillo-Garza, G. L. Klimchitskaya, V. M. Mostepanenko, and U. Mohideen, *Phys. Rev. B* **85**, 165443 (2012).
 - [36] R. S. Decca, D. López, E. Fischbach, G. L. Klimchitskaya, D. E. Krause, and V. M. Mostepanenko, *Phys. Rev. D* **75**, 077101 (2007).
 - [37] R. S. Decca, D. López, E. Fischbach, G. L. Klimchitskaya, D. E. Krause, and V. M. Mostepanenko, *Eur. Phys. J. C* **51**, 963 (2007).
 - [38] B. A. Dobrescu and I. Mocioiu, *JHEP* **0611**, 005 (2006).
 - [39] L. Hunter, J. Gordon, S. Peck, D. Ang, and J.-F. Lin, *Science* **339**, 928 (2013).
 - [40] M. Bordag, B. Geyer, G. L. Klimchitskaya, and V. M. Mostepanenko, *Phys. Rev. D* **62**, 011701(R) (2000).
 - [41] R. S. Decca, E. Fischbach, G. L. Klimchitskaya, D. E. Krause, D. López, and V. M. Mostepanenko, *Phys. Rev. D* **79**, 124021 (2009).
 - [42] A. A. Banishev, C.-C. Chang, G. L. Klimchitskaya, V. M. Mostepanenko, and U. Mohideen, *Phys. Rev. B* **85**, 195422 (2012).
 - [43] E. Fischbach, G. L. Klimchitskaya, D. E. Krause, and V. M. Mostepanenko, *Eur. Phys. J. C* **68**, 223 (2010).

- [44] J. M. Obrecht, R. J. Wild, M. Antezza, L. P. Pitaevskii, S. Stringari, and E. A. Cornell, *Phys. Rev. Lett.* **98**, 063201 (2007).
- [45] V. B. Bezerra, G. L. Klimchitskaya, V. M. Mostepanenko, and C. Romero, *Phys. Rev. D* **83**, 075004 (2011).
- [46] Y. Bao, R. Guérout, J. Lussange, A. Lambrecht, R. A. Cirelli, F. Klemens, W. M. Mansfield, C. S. Pai, and H. B. Chan, *Phys. Rev. Lett.* **105**, 250402 (2010).
- [47] R. S. Decca, D. López, E. Fischbach, D. E. Krause, and C. R. Jamell, *Phys. Rev. Lett.* **94**, 240401 (2005).
- [48] V. M. Mostepanenko and G. L. Klimchitskaya, *Int. J. Mod. Phys. A* **25**, 2302 (2010).
- [49] R. O. Behunin, F. Intravaia, D. A. R. Dalvit, P. A. Maia Neto, and S. Reynaud, *Phys. Rev. A* **85**, 012504 (2012).
- [50] A. O. Sushkov, W. J. Kim, D. A. R. Dalvit, and S. K. Lamoreaux, *Nature Phys.* **7**, 230 (2011).
- [51] D. Garcia-Sanchez, K. Y. Fong, H. Bhaskaran, S. Lamoreaux, and H. X. Tang, *Phys. Rev. Lett.* **109**, 027202 (2012).
- [52] V. B. Bezerra, G. L. Klimchitskaya, U. Mohideen, V. M. Mostepanenko, and C. Romero, *Phys. Rev. B* **83**, 075417 (2011).
- [53] G. L. Klimchitskaya and V. M. Mostepanenko, *Int. J. Mod. Phys. A* **26**, 3944 (2011).
- [54] G. L. Klimchitskaya, M. Bordag, E. Fischbach, D. E. Krause, and V. M. Mostepanenko, *Int. J. Mod. Phys. A* **26**, 3918 (2011).
- [55] G. L. Klimchitskaya, M. Bordag, and V. M. Mostepanenko, *Int. J. Mod. Phys. A* **27**, 1260012 (2012).
- [56] M. Bordag, G. L. Klimchitskaya, and V. M. Mostepanenko, *Phys. Rev. Lett.* **109**, 199701 (2012).
- [57] B. Geyer, G. L. Klimchitskaya, and V. M. Mostepanenko, *Phys. Rev. B* **81**, 104101 (2010).
- [58] G. L. Klimchitskaya, B. Geyer, and V. M. Mostepanenko, *Int. J. Mod. Phys. A* **25**, 2293 (2010).
- [59] C. C. Speake and C. Trenkel, *Phys. Rev. Lett.* **90**, 160403 (2003).
- [60] R. Decca and G. Voisin, *APS Bulletin* **58**, R41.00008 (2013).
- [61] H.-C. Chiu, G. L. Klimchitskaya, V. N. Marachevsky, V. M. Mostepanenko, and U. Mohideen, *Phys. Rev. B* **80**, 121402(R) (2009).
- [62] H.-C. Chiu, G. L. Klimchitskaya, V. N. Marachevsky, V. M. Mostepanenko, and U. Mohideen,

Phys. Rev. B **81**, 115417 (2010).

[63] A. P. Prudnikov, Yu. A. Brychkov, and O. I. Marichev, *Integrals and Series* (Gordon and Breach, New York, 1986), Vol. 1.

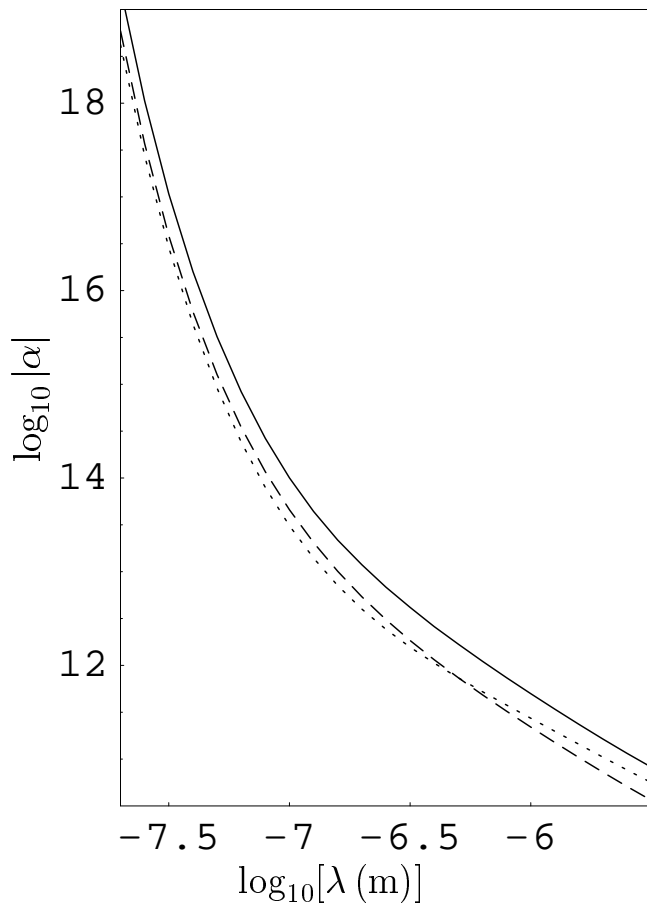


FIG. 1: Constraints on the parameters of Yukawa-type corrections to Newton's gravitational law obtained in this work from measurement of the gradient of the Casimir force between two Ni surfaces (solid line), between two Au surfaces (dashed line) and between an Au and a Ni surfaces (dotted line). Here and in Figs. 2, 4 the regions of (λ, α) plane below each line are allowed and above each line are prohibited (see text for further discussion).

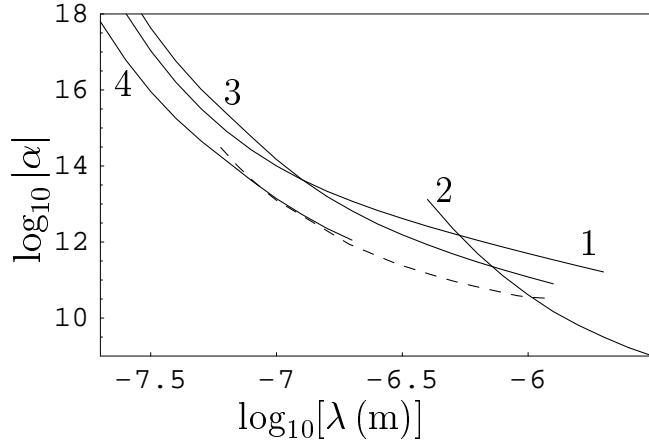


FIG. 2: Constraints on the parameters of Yukawa-type corrections to Newton’s gravitational law obtained in this work (solid line 1), in Ref. [26] from measurements of the thermal Casimir-Polder force [44] (solid line 2), in Ref. [45] from measurements of the gradient of the Casimir force between metallic and corrugated semiconductor surfaces [46] (solid line 3), in Refs. [36, 37] from measurements of the gradient of the Casimir force between two metallic surfaces (solid line 4), and in Ref. [47] from the Casimir-less experiment (dashed line).

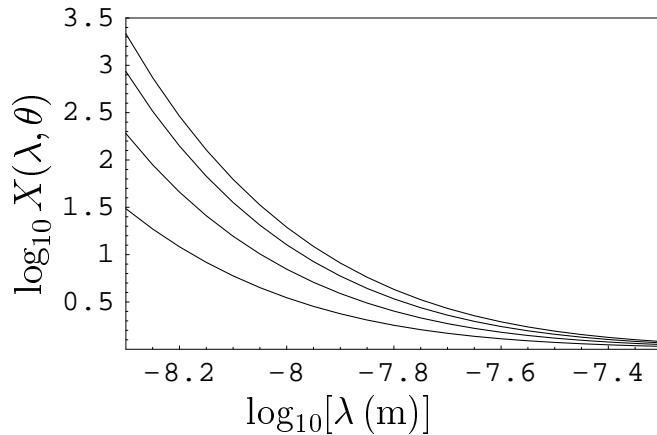


FIG. 3: The quantity $X(\lambda, \theta)$ defined in Eq. (16) is plotted by the solid lines as a function of λ at $\theta = 0^\circ, 1.2^\circ, 1.8^\circ,$ and 2.4° from bottom to top, respectively.

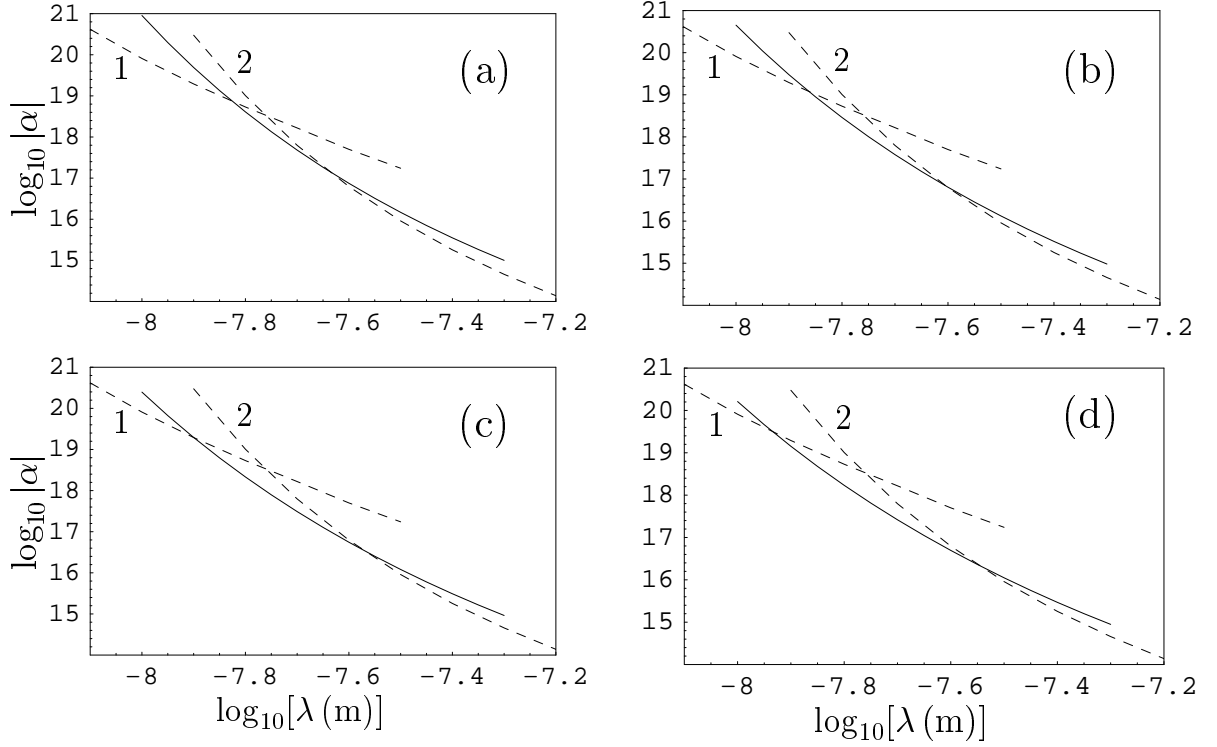


FIG. 4: Constraints on the parameters of Yukawa-type corrections to Newton’s gravitational law obtained in this work (solid line), in Ref. [26] from measurements of the lateral Casimir force between sinusoidally corrugated surfaces [61, 62] (dashed line 1), and from effective measurements of the Casimir pressure between metallic plates by means of a micromachined oscillator [36, 37] (dashed line 2). The angle between the axes of corrugations is equal to (a) $\theta = 0^\circ$, (b) $\theta = 1.2^\circ$, (c) $\theta = 1.8^\circ$, and (d) $\theta = 2.4^\circ$.

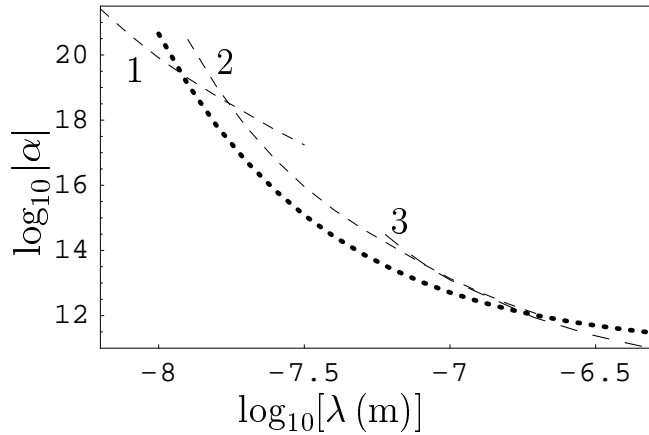


FIG. 5: Prospective constraints on the parameters of Yukawa-type corrections to Newton's gravitational law which can be obtained from dynamic measurement of the gradient of the Casimir force between sinusoidally corrugated surfaces are shown by the dotted line. For comparison purposes the dashed lines 1, 2, and 3 indicate the strongest current constraints obtained in Ref. [26] from measurements of the lateral Casimir force between sinusoidally corrugated surfaces [61, 62], from effective measurements of the Casimir pressure between metallic plates by means of a micromachined oscillator [36, 37], and in Ref. [47] from the Casimir-less experiment, respectively.